



MEaSURES Greenland Quarterly Ice Sheet Velocity Mosaics from SAR and Landsat, Version 4

USER GUIDE

How to Cite These Data

As a condition of using these data, you must include a citation:

Joughin, I. 2022. *MEaSURES Greenland Quarterly Ice Sheet Velocity Mosaics from SAR and Landsat, Version 4*. [Indicate subset used]. Boulder, Colorado USA. NASA National Snow and Ice Data Center Distributed Active Archive Center. <https://doi.org/10.5067/BGBF7KY84Q2N>. [Date Accessed].

Literature Citation

As a condition of using these data, we request that you acknowledge the author(s) of this data set by referencing the following peer-reviewed publications.

Joughin, I., B. Smith, I. Howat, T. Scambos, and T. Moon. 2010. Greenland flow variability from ice-sheet-wide velocity mapping, *Journal of Glaciology*. 56. 415-430.

<https://doi.org/10.3189/002214310792447734>

Joughin, I., B. Smith, and I. Howat. 2018. Greenland Ice Mapping Project: ice flow velocity variation at sub-monthly to decadal timescales, *The Cryosphere*. 12. 2211-2227. <https://doi.org/10.5194/tc-12-2211-2018>

FOR QUESTIONS ABOUT THESE DATA, CONTACT NSIDC@NSIDC.ORG

FOR CURRENT INFORMATION, VISIT <https://nsidc.org/data/NSIDC-0727>



National Snow and Ice Data Center

TABLE OF CONTENTS

1	DATA DESCRIPTION.....	2
1.1	Parameters	2
1.2	File Information	2
1.2.1	Format	2
1.2.2	File Contents	2
1.2.3	Naming Convention	3
1.3	Spatial Information	5
1.3.1	Coverage	5
1.3.2	Resolution.....	5
1.3.3	Geolocation	6
1.4	Temporal Information.....	7
1.4.1	Coverage	7
1.4.2	Resolution.....	7
2	DATA ACQUISITION AND PROCESSING	7
2.1	Acquisition.....	7
2.1.1	Annual Variation in Data Acquisition	7
2.2	Processing	8
2.3	Baseline Fits	9
2.3.1	Aggregation and Weighting.....	9
2.3.2	Submergence/Emergence Velocity	10
2.3.3	Temporal Offset Calculation.....	10
2.3.4	Interpolated Points	11
2.3.5	Areas with No Data	11
2.3.6	GDAL-Generated Cloud Optimized GeoTIFFs	11
2.4	Quality, Errors, and Limitations	11
2.5	Instrumentation	13
3	SOFTWARE AND TOOLS.....	13
4	VERSION HISTORY	13
5	RELATED DATA SETS	14
6	RELATED WEBSITES.....	14
7	CONTACTS AND ACKNOWLEDGMENTS.....	15
7.1	Contacts.....	15
7.2	Acknowledgments.....	15
8	REFERENCES	15
9	DOCUMENT INFORMATION.....	16
9.1	Publication Date.....	16
9.2	Date Last Updated	16


1 DATA DESCRIPTION

This data set, part of the NASA Making Earth System Data Records for Use in Research Environments (MEaSUREs) program, contains quarterly ice velocity mosaics for the Greenland Ice Sheet posted at 200 m. Velocities are estimated using Synthetic Aperture Radar (SAR) data from TerraSAR-X/TanDEM-X (TSX/TDX) and Sentinel-1A and -1B and optical imagery from Landsat 8.

1.1 Parameters

Velocities are reported in meters per year and provided as velocity magnitude (v_v), x and y component velocities (v_x , v_y), and x and y component velocity error estimates (e_x , e_y).

In addition, a temporal offset parameter (dT) is included that reports the difference in days between the date of each velocity estimate and the midpoint date of the corresponding measurement period.

 Because of the data aggregation process, the true date represented by the data may differ from the nominal midpoint date of the measurement period. As such, dT provides a metric to assess potential temporal skew in the data (See “Section 2.3.3 | Temporal Offset Calculation” for details.).

1.2 File Information

1.2.1 Format

Data are provided as cloud optimized GeoTIFFs (.tif) and shapefiles. TIFF and JPEG browse files are also available.

1.2.2 File Contents

Data files are available for each quarter (i.e., three month period) in the data record. Quarters span:

- 1 December – 28 (or 29) February
- 1 March – 31 May
- 1 June – 31 August
- 1 September – 30 November

Each of the parameters listed in the “Parameters” section above is provided as a separate, quarterly GeoTIFF file. Quarterly shapefiles are also available that indicate the source of the image pairs (SAR or Landsat 8) used to produce the mosaics.

1.2.3 Naming Convention

1.2.3.1 GeoTIFF

Naming Convention:

[product name]_[start date]_[end date]_[parameter]_[version].[ext]

Example:

GL_vel_mosaic_Quarterly_01Dec14_28Feb15_vv_v04.0.tif

GL_vel_mosaic_Quarterly_01Dec14_28Feb15_vx_v04.0.tif

GL_vel_mosaic_Quarterly_01Dec14_28Feb15_vy_v04.0.tif

GL_vel_mosaic_Quarterly_01Dec14_28Feb15_ex_v04.0.tif

GL_vel_mosaic_Quarterly_01Dec14_28Feb15_ey_v04.0.tif

GL_vel_mosaic_Quarterly_01Dec14_28Feb15_dT_v04.0.tif

The following table describes the variables in the GeoTIFF file naming convention:

Table 1. GeoTIFF File Naming Convention

Variable Name	Description
product name	GL_vel_mosaic_Quarterly (Greenland Quarterly Ice Sheet Velocity Mosaics)
start date	Start date of measurement period (DDMMYY)
end date	End date of measurement period (DDMMYY)
parameter	One of the following: vv (velocity magnitude) vx, vy (component velocity) ex, ey (component velocity error) dT (temporal offset)
version	Two digit version, plus release number (when applicable). E.g., V04.0 = Version 4 (initial release).

Variable Name	Description
ext	File extension (.tif)

1.2.3.2 Shapefile

Naming Convention:

[product name]_[start date]_[end date]_[source]_[version].[ext]

Example:

- GL_vel_mosaic_Quarterly_01Dec14_28Feb15_LS8_v04.0.dbf
- GL_vel_mosaic_Quarterly_01Dec14_28Feb15_LS8_v04.0.prj
- GL_vel_mosaic_Quarterly_01Dec14_28Feb15_LS8_v04.0.shp
- GL_vel_mosaic_Quarterly_01Dec14_28Feb15_LS8_v04.0.shx

The following table describes the variables in the shapefile file naming convention:

Table 2. Shapefile File Naming Convention

Variable Name	Description
product name	GL_vel_mosaic_Quarterly (Greenland Quarterly Ice Sheet Velocity Mosaics)
start date	Start date of measurement period (DDMMYY)
end date	End date of measurement period (DDMMYY)
source	SAR or LS8 (Landsat 8)
version	Two digit version, plus release number (when applicable). E.g., V04.0 = Version 4 (initial release).

Variable Name	Description
ext	File extension. For this data set, a complete shapefile consists of four file types: <ul style="list-style-type: none"> .dbf (dBASE table file) .shp (main file) .shx (index file) .prj (projection definition file)

1.2.3.3 Browse Images

Browse images follow the same naming convention described above, but include the word "browse" in the file name and either the "tif" or "jpg" file extension. For example:

GL_vel_mosaic_Quarterly_01Dec14_28Feb15_browse_v04.0.jpg

GL_vel_mosaic_Quarterly_01Dec14_28Feb15_browse_v04.0.tif

1.3 Spatial Information

1.3.1 Coverage

Data span the Greenland Ice Sheet as follows:

Northernmost Latitude: 83° N

Southernmost Latitude: 58.5° N

Eastermost Longitude: 8.32° W

Westernmost Longitude: 90.9° W

1.3.2 Resolution

Data are posted at 200 m.

Note that this resolution does not reflect the true "on the ground" resolution. The velocities are derived from source data with spatially varying averages that range from a few hundred meters to 1.5 km, making it difficult to specify the resolution at any point.

For example, some estimates represent the average of 30 or more individual measurements. While this enhances the final resolution to some degree relative to the individual source products, the amount is not well quantified.

For work requiring finer resolution, users may prefer the individual DLR TerraSAR-X (TSX)/TanDEM-X (TDX) and USGS Landsat data where available (see [MEaSURES Greenland Ice Velocity: Selected Glacier Site Velocity Maps from InSAR](#) and [MEaSURES Greenland Ice Velocity: Selected Glacier Site Velocity Maps from Optical Images](#)).

1.3.3 Geolocation

The following tables provide information about geolocating this data set. Velocity-related GeoTIFFs are provided in the NSIDC Sea Ice Polar Stereographic North projection (see Table 3). Shapefiles are geolocated with WGS 84 latitudes and longitudes (see Table 4).

Table 3. NSIDC Sea Ice Polar Stereographic North (EPSG:3413)

Geographic Coordinate System	WGS 84
Projected Coordinate System	WGS 84 / NSIDC Sea Ice Polar Stereographic North
Longitude of True Origin	-45
Latitude of True Origin	70
Scale factor at longitude of true origin	1
Datum	WGS 1984
Ellipsoid/spheroid	WGS 84
Units	meter
False Easting	0
False Northing	0
EPSG Code	3413
PROJ4 String	+proj=stere +lat_0=90 +lat_ts=70 +lon_0=-45 +k=1 +x_0=0 +y_0=0 +datum=WGS84 +units=m +no_defs
Reference	http://epsg.io/3413

Table 4. World Geodetic System 1984 (EPSG:4326)

Geographic Coordinate System	WGS 84
Projected Coordinate System	N/A
Longitude of True Origin	0°
Latitude of True Origin	N/A
Scale factor at longitude of true origin	N/A
Datum	World Geodetic System 1984
Ellipsoid/spheroid	WGS 84
Units	degree
False Easting	N/A

False Northing	N/A
EPSG Code	4326
PROJ4 String	+proj=longlat +datum=WGS84 +no_defs
Reference	http://epsg.io/4326

1.4 Temporal Information

1.4.1 Coverage

1 December 2014 to 28 February 2022

1.4.2 Resolution

Quarterly:

- 1 December – 28 (or 29) February
- 1 March – 31 May
- 1 June – 31 August
- 1 September – 30 November

2 DATA ACQUISITION AND PROCESSING

2.1 Acquisition

The velocity mosaics in this data set were produced from data acquired by the European Space Agency (ESA) Sentinel-1A and Sentinel-1B satellites, supplemented with TSX/TDX data for coastal outlets. The data were acquired in either 12-day (through Sept 2016) or 6-day repeat cycles (October 2016 forward). In cases of missing acquisitions, the repeat periods may be longer (integer multiples of 6 or 12 days) for some of the image pairs. In addition, USGS's Landsat 8 velocities were merged with SAR data during periods with sufficient daylight.

2.1.1 Annual Variation in Data Acquisition

2015 (Dec 1, 2014 – Nov 30, 2015)

Sentinel-1A data acquisitions began in 2015, but the acquisition rates were not as regular as in later years. As a result, these data tend to be somewhat noisier than the 2016 data, particularly in the middle of the ice sheet. In addition, the sampling of coastal regions is more irregular (there are gaps in the temporal coverage where TSX/TDX data were not acquired by the satellite for a month or more), which reduces the averaging of seasonal variation.

2016 (Dec 1, 2015 – Nov 30, 2016)

For this year, the six Sentinel-1A tracks that image the majority of the Greenland coast were collected for almost every 12-day satellite repeat cycle. Beginning in October 2016, Sentinel-1B started acquiring data over Greenland in an orbit that lags Sentinel-1A by six days, providing better coverage and thus more correlations in the data. As a result, accuracy for these mosaics is considerably better than the mosaics for 2015 for most regions.

2017 (Dec 1, 2016 – Nov 30, 2017)

These products are similar to the earlier 2015 and 2016 products. The major difference is that this is the first year that regular 6-day coverage occurred throughout the year, which should improve performance on fast moving glaciers. In addition, the Copernicus Sentinel mission improved coverage for the southern part of Greenland in mid-2017, so the results should be improved for areas south of 67.5 degrees.

2018 (Dec 1, 2017 – Nov 30, 2018)

These products follow the same specifications as the previous year's release, with the following minor differences: some data using a few scenes from the COntellation of small Satellites for the Mediterranean basin Observation (COSMO-SkyMed) were included; some of the glaciers which were monitored by TSX in past years are covered by other instruments during this year.

2019 (Dec 1, 2018 – Nov 30, 2021)

No changes. See specifications for previous releases.

2.2 Processing

These mosaics were computed as averages of all available data at each point, weighted by their respective errors following Joughin, 2002. Whereas prior versions were based entirely on speckle/feature tracking, Version 4 incorporates interferometric phase when possible, to improve accuracy (Joughin et al., 2017).

With Sentinel-1 TOPS mode, azimuth motion introduces phase discontinuities at burst boundaries (roughly every 20 km) because the radar squint angles differ at the fore and aft edges of each burst. These errors were corrected by using an existing velocity map to model and remove burst discontinuities similar to the procedure described by Andersen et al. (2020). Phase discontinuities introduced by the ionosphere were reduced by processing the interferograms using the InSAR Computing Environment (ISCE) with the ionospheric correction enabled (Fattahi et al., 2017).

❗ For non-winter quarters, little if any phase data is included in the solution because most phase data are concentrated during December to February. While the inclusion of phase data in certain areas during these quarters does reduce errors substantially relative to earlier versions, the overall impact to the quarterly data product is sporadic.

2.3 Baseline Fits

Each azimuth and range offset swath product used to produce the mosaics must be calibrated to determine parameters related to the relative positions of the satellites when the images in a pair were collected (e.g., baseline). In previous versions of this data set, linear regressions were used to fit control points with known velocity and elevation and thus capture the along-track variation in the parameters. However, this approach can propagate any biases present in the control points.

With Sentinel-1 greater reliance can be placed on the knowledge of the parameters derived from the orbital state vectors. As a result, the data in Version 4 have been re-calibrated relative to previous versions by using the fitting process to determine a constant for each parameter rather than a quadratic function, with the along-track dependence determined directly from the state vectors.

For periods where data are not well controlled (sparse ground control points), control points from other periods with adequate controls are used. This greatly improves consistency of the data from quarter to quarter. While this could mask some true change, the errors without this procedure are far larger than any change likely to occur.

2.3.1 Aggregation and Weighting

For each quarter, all available data are aggregated and combined in an error-weighted method to achieve an optimal estimate with respect to error reduction. However, due to limited coverage or lack of unsuccessful matches, there are data gaps such that the full three month period may not be sampled uniformly.

In order to maximize coverage, data were included where the sampling interval of the input data did not fully lie within the output interval. In these cases, the data are weighted by the amount they overlap the output interval (e.g., if the first 6 days of a 12-day image pair lie within the output interval, a weight of 0.5 would be applied). If uniformly sampled data, e.g., every 12 days, and uniformly weighted data were combined, this procedure would be equivalent to a linear interpolation of the time series.

Finally, to reduce error and improve coverage, data were also included where the input estimate spanned an interval longer than the output interval (e.g., up to a five month pair for the three month

output). This inclusion slightly degrades the temporal resolution, but improves coverage and helps reduce errors. Weights are applied to data spanning more than three months to deemphasize their contribution, such that they only factor into estimates where coverage from other data is poor. As such, while the nominal, three month resolution is valid for most of the data set, the actual resolution can be lower in some regions.

2.3.2 Submergence/Emergence Velocity

In previous versions, velocities were computed using a surface-parallel flow assumption to estimate and remove the vertical velocity contribution to the line-of-sight displacement so that the horizontal velocities can be resolved (Joughin et al., 1998). This assumption, however, neglects the submergence/emergence velocity (i.e., the vertical motion of the ice surface).

Version 4 has been corrected using an ice-equivalent submergence/emergence velocity based on a 30-year estimate of surface mass balance (net accumulation after ablation for 1991-2020) derived from MAR (v3.11) regional climate model (Fettweis et al., 2017).

2.3.3 Temporal Offset Calculation

As a measure of temporal skew, the mean temporal offset dT was calculated from the midpoint date in days for each point. This metric is calculated by applying the same weighting to the difference between the date for each velocity estimate and the midpoint date and then weighted using the same methods as the velocity data. In estimating velocity, different weights are used for the v_x and v_y components, so an intermediate weight is used for the individual dT s. In the final mosaicking step, any data with dT greater than one-half the output interval was discarded. As a result, the time stamp error for the quarterly product is less than or equal to approximately 45 days.

In more detail, the process for calculating dT follows these steps:

1. Using a Day of the Year (DOY) calendar, determine the midpoint for the measurement period i.e., quarterly, monthly or annual.
2. For each pixel, identify the image pairs used as input for velocity and calculate the central date in terms of the DOY.
3. Calculate a weighted average central date for that pixel using an intermediate weight based on the weights used for the v_x and v_y components.
4. $dT = \text{weighted average central date} - \text{midpoint}$.

Although the averaged dT value provides some idea of the deviation from nominal date, users should be cautious when using dT to correct dates.

For example, for a quarterly mosaic that covers the period 1 March – 31 May, the nominal center date is 15 April. If $dT = 10$, then 25 April would better represent the midpoint date for the parameters in this interval.

However, there are convoluted cases that could also result in $dT = 10$. For example, say the mosaic was produced using images collected from 13–24 March and 5–18 to May. In this case, dT would equal 10 with no measurement from April 25. Alternatively, a mosaic produced using a single pair from 20–30 April would also have $dT = 10$, but with a sample from April 25.

The data providers recommend using dT to flag potential time skew issues, rather than for date correction. In cases where a large temporal skew exists, other GrIMP products with finer temporal sampling are likely better suited for analyzing temporally varying behavior.

2.3.4 Interpolated Points

Small gaps in the final maps have been filled via interpolation. These points can be identified as those that have valid velocity data but no corresponding error estimate. See Joughin et al. (2002) for more detail on errors and how they were computed.

2.3.5 Areas with No Data

Areas with no data correspond either to regions where no data were acquired or where the interferometric or optical correlation was insufficient to produce an estimate. This occurs most often in areas with high snow accumulation. The no data value for vv , ex , and ey files is -1 . The no data value for vx , vy , and dT is $-2e9$.

2.3.6 GDAL-Generated Cloud Optimized GeoTIFFs

The GeoTIFFs were generated using Geospatial Data Abstraction Library (GDAL), to make them compatible with the latest cloud optimized GeoTIFF format. GDAL generates previews for Cloud Optimized GeoTIFFs; however, the software uses cubic interpolation that results in minor artifacts around the lower resolution previews. Averaging is used to avoid this issue.

 When GDAL creates cloud optimized GeoTIFFs, it writes image statistics directly to the file header.

2.4 Quality, Errors, and Limitations

Recalibrations used to create this data set substantially improve the accuracy of the products, especially in the interior of the ice sheet, with errors well under 1 m/yr. However, as with previous versions, these data do not represent true quarterly averages due to the weighting schemes. For

example, in some places mid-summer may be weighted more heavily than mid-winter due to the seasonal availability of Landsat 8 data. Similarly, clouds or large snow accumulation events may affect the seasonal distribution of the data.

As a result, these data should not be used to determine inter-annual change for interior regions of the ice sheet (roughly defined as areas above 2,000 m). In outlet glaciers close to the coast where the baselines are well constrained by bedrock, the velocity mosaics are better suited to this task. However, care should be exercised in interpreting any change observed in intermediate regions (roughly 1000 m to 2000 m), i.e., avoid areas where the observed changes seem to follow a satellite swath boundary (Refer to Figure 5 in Phillips et al., 2013, for an example.).

In general, the error estimates represent the average behavior of the data. This means that errors may be much lower than reported in some areas and much greater in others; care should be taken when assigning statistical significance based on the errors, especially given that the errors can be correlated over large areas. For example, even if the errors are correct in a global sense, one might compare two mosaics and find a large difference over 5% of the ice sheet. However, because errors can be spatially correlated over broad areas, one should not assume significance at the 95% confidence level; this might be precisely the 5% that statistically should exceed the errors because the errors are not uniformly distributed. By contrast, if the errors were completely uncorrelated one could average over neighborhoods to reduce the error.

While the data are posted at 200 m, the true resolution varies between a few hundred meters to 1.5 km. *Posting* represents the spacing between samples and should not be confused with the resolution at which the data were collected. Many small glaciers are resolved outside the main ice sheet, but for narrow (<1 km) glaciers, the velocity represents an average of both moving ice and stationary rock. As a result, while the glacier may be visible in the map, the actual speed may be underestimated. For smaller glaciers, interpolation produces artifacts where the interpolated value is derived from nearby rock, causing apparent stationary regions in the middle of otherwise active flow. The data have been screened to remove most of these artifacts, but should be used with caution.

In areas where Sentinel-1A and -1B ascending and descending crossing orbit data were available, an error-weighted range-offset-only solution was included in the velocity algorithm. Where these data are included, the errors are generally substantially lower than solutions with azimuth offsets, which can be subject to large errors due to ionospheric streaking. However, by virtue of the error weighting, the range-offset-only solutions tend to dominate the aggregate output and yield more accurate results.

Regarding the correction for ice-equivalent submergence/emergence velocity, recent increases in melt may impact these estimates. However, this parameter should evolve at decadal or greater timescales for much of the ice sheet.

In addition, this correction does not account for firn compaction due to the large uncertainties in penetration depth and compaction rates. For the bare-ice zone, where the correction tends to be the largest, this omission should have no effect. For firn covered areas, the correction may underestimate the true submergence/emergence velocity by up to a few tens of centimeters per year. However, the results still represent an overall improvement in accuracy.

Finally, this product uses a variation of the GrIMP DEM (see [NSIDC-0715](#)) which has a lower resolution of 270 m and utilizes geoidal heights for the ocean. The DEM also contains a correction to a 15m horizontal shift that was identified previously.

2.5 Instrumentation

- European Space Agency (ESA)
 - [Sentinel-1](#)
- Deutsches Zentrum für Luft- und Raumfahrt (DLR)
 - [TerraSAR-X \(TSX\)](#)
 - [TanDEM-X \(TDX\)](#)
- U.S. Geological Survey (USGS)
 - [Landsat 8](#)

3 SOFTWARE AND TOOLS

GeoTIFF files and shapefiles can be viewed with a variety of Geographical Information System (GIS) software packages including [QGIS](#) and [ArcGIS](#).

4 VERSION HISTORY

Table 5. Version History Summary

Version	Release Date	Description of Changes
4.0	April 24, 2023	<ul style="list-style-type: none"> • Version 4 retired (superceded by Version 5).
4.0	August 2022	<ul style="list-style-type: none"> • Temporal coverage extended • Data recalibrated relative to previous versions to reduces biases imposed by quadratic fits to control points • Correction added for the submergence/emergence velocity • Addition of interferometric phase data where available.

Version	Release Date	Description of Changes
3.0	June 2021	<ul style="list-style-type: none"> • Use of GDAL 3.2.1 to create cloud optimized GeoTIFFs • Update of temporal coverage • Data reprocessed utilizing a corrected DEM. See user note in section 2.2
2.0	December 2020	<ul style="list-style-type: none"> • New file naming convention • Data set temporal range increased by one year from: 01 December 2014 to 30 November 2019. • Application of a new DEM, NSIDC-0715; prior versions relied on NSIDC-0646 • All files have a 200 m resolution with the exception of the browse.jpg which is at 500 m; 500 m resolution velocity files no longer available • A more rigorous culling of the data removed bad data and added previously overlooked data. As a result, mosaics show more areas with no data, the min/max ex and ey values are lower, and SAR/LS8 feature counts differ from Version 1. • The no data value for vv changed from -0.1 to -1; the no data value for ex and ey changed from -2e9 to -1. • Newly available are cloud optimized GeoTIFFs along with tif.aux.xml, and jpg.aux.xml files.
1.1	October 2019	Updated .tif file names within .vrt files to match the actual .tif file names
1.0	February 2018	Initial release

5 RELATED DATA SETS

- [MEaSURES Greenland Annual Ice Sheet Velocity Mosaics from SAR and Landsat](#)
- [MEaSURES Greenland Monthly Ice Sheet Velocity Mosaics from SAR and Landsat](#)
- [MEaSURES Greenland Ice Velocity: Selected Glacier Site Velocity Maps from InSAR](#)
- [MEaSURES Greenland Ice Sheet Velocity Map from InSAR](#)
Data<https://nsidc.org/data/nsidc-0478>

6 RELATED WEBSITES

- [MEaSURES Data | Overview](#)
- [Alaska Satellite Facility](#)
- [Greenland Ice Sheet Mapping Project \(GrIMP\)](#)

7 CONTACTS AND ACKNOWLEDGMENTS

7.1 Contacts

Ian Joughin

University of Washington

Applied Physics Laboratory

7.2 Acknowledgments

This project was supported by a grant from the NASA Making Earth System Data Records for Use in Research Environments ([MEaSUREs](#)) Program.

8 REFERENCES

Andersen, J. K., A. Kusk, J.P.M. Boncori, C.S. Hvidberg, and A. Grinsted. (2020). Improved Ice Velocity Measurements with Sentinel-1 TOPS Interferometry. *Remote Sens*, 12, 2014.

<https://doi.org/10.3390/rs12122014>.

Fattahi, H., M. Simons, and P. Agram. (2017). InSAR Time-Series Estimation of the Ionospheric Phase Delay: An Extension of the Split Range-Spectrum Technique. *IEEE T Geosci Remote*, 55, 5984–5996. <https://doi.org/10.1109/tgrs.2017.2718566>.

Fettweis, X., J.E. Box, C. Agosta, C. Amory, C. Kittel, C. Lang, D. van As, H. Machguth, and H. Gallée. (2017). Reconstructions of the 1900–2015 Greenland ice sheet surface mass balance using the regional climate MAR model. *Cryosphere*, 11, 1015–1033, <https://doi.org/10.5194/tc-11-1015-2017>.

Joughin, I., R. Kwok, and M. Fahnestock. (1998). Interferometric estimation of three-dimensional ice-flow using ascending and descending passes. *IEEE*, 36, 25–37, 1998.

<https://doi.org/10.1109/36.655315>

Joughin, I. (1995). Estimation of ice-sheet topography and motion using interferometric synthetic aperture radar. *PhD Dissertation*, University of Washington.

Joughin, I. (2002). Ice-sheet velocity mapping: a combined interferometric and speckle-tracking approach. *Annals of Glaciology*, 34, 195–201. <https://doi.org/10.3189/172756402781817978>

Joughin, I., Tulaczyk, S., Bindschadler, R., & Price, S. F. (2002). Changes in west Antarctic ice stream velocities: Observation and analysis. *Journal of Geophysical Research: Solid Earth*, 107(B11), EPM 3-1-EPM 3-22. <https://doi.org/10.1029/2001jb001029>

- Joughin, I., Abdalati, W., & Fahnestock, M. (2004). Large fluctuations in speed on Greenland's Jakobshavn Isbræ glacier. *Nature*, 432(7017), 608–610. <https://doi.org/10.1038/nature03130>
- Joughin, I., Smith, B. E., Howat, I. M., Scambos, T., & Moon, T. (2010). Greenland flow variability from ice-sheet-wide velocity mapping. *Journal of Glaciology*, 56(197), 415–430. <https://doi.org/10.3189/002214310792447734>
- Joughin, I., Smith, B. E., & Howat, I. M. (2017). A complete map of Greenland ice velocity derived from satellite data collected over 20 years. *Journal of Glaciology*, 64(243), 1–11. <https://doi.org/10.1017/jog.2017.73>
- Moon, T., & Joughin, I. (2008). Changes in ice front position on Greenland's outlet glaciers from 1992 to 2007. *Journal of Geophysical Research*, 113(F2). <https://doi.org/10.1029/2007jf000927>
- Phillips, T., Rajaram, H., Colgan, W., Steffen, K., & Abdalati, W. (2013). Evaluation of cryo-hydrologic warming as an explanation for increased ice velocities in the wet snow zone, Sermeq Avannarleq, West Greenland. *Journal of Geophysical Research: Earth Surface*, 118(3), 1241–1256. <https://doi.org/10.1002/jgrf.20079>
- Rignot, E. (2006). Changes in the Velocity Structure of the Greenland Ice Sheet. *Science*, 311(5763), 986–990. <https://doi.org/10.1126/science.1121381>

9 DOCUMENT INFORMATION

9.1 Publication Date

August 2022

9.2 Date Last Updated

April 2023